

# SPRAY-DRYING CELLULOSE NANOFIBRILS: EFFECT OF DRYING PROCESS PARAMETERS ON PARTICLE MORPHOLOGY AND SIZE DISTRIBUTION

*Yucheng Peng*<sup>†</sup>

Graduate Research Assistant  
E-mail: yucheng.peng@maine.edu

*Yousoo Han*

Assistant Research Professor  
E-mail: yousoo.han@umit.maine.edu

*Douglas J. Gardner*<sup>\*†</sup>

Professor of Wood Science and Technology  
AEWC Advanced Structures and Composites Center  
School of Forest Resources  
University of Maine  
Orono, ME 04469-5793  
E-mail: douglasg@maine.edu

(Received May 2012)

**Abstract.** Spray-drying was chosen as an appropriately scalable manufacturing method to dry cellulose nanofibril (CNF) suspensions. Spray-drying of two different types of CNF suspensions—nanofibrillated cellulose (NFC) and cellulose nanocrystals (CNC)—was carried out using a laboratory-scale spray dryer. Effects of three spray-drying process parameters on particle morphology and particle size distribution were evaluated: 1) gas flow rate; 2) liquid feed rate; and 3) suspension solids concentration. Particle morphology was characterized by scanning electron microscopy (SEM) and a morphology analyzer. SEM showed that spray-drying of NFC formed fibrous particles and fibrous agglomerates, whereas spray-drying CNCs produced spherical and mushroom cap (or donut)-shaped particles. Particle morphology formation mechanisms are proposed for spray-drying nanocellulose suspensions. The effect of the three spray-drying process parameters on particle size distribution depended on the drying nature of the materials. The three parameters interacted to significantly affect particle size of CNC suspensions, whereas they did not interact to affect particle size of NFC suspensions. For the CNC suspension, a higher gas flow rate produced smaller particle sizes. The gas flow rate did not affect particle size for NFC suspensions. The effect of liquid feed rate and solids concentration on CNF particle size was negligible in this study. The smallest mean circle equivalent diameters produced in this study were 3.95  $\mu\text{m}$  for NFC and 3.64  $\mu\text{m}$  for CNC.

**Keywords:** Nanocellulose, spray-drying, particle morphology, particle size distribution.

## INTRODUCTION

The intensive research of cellulose nanofibrils (CNF) and their application as a reinforcing component in polymer composites have received considerable attention (Beecher 2007; Hubbe et al 2008; Eichhorn et al 2010; Habibi et al 2010; Siro and Plackett 2010; Siqueira et al 2010; Klemm et al 2011; Moon et al 2011). Because

of their hydrophilic nature and propensity to agglomerate, a major processing challenge is to properly dry CNF from aqueous suspensions (Gardner et al 2008). In a previous study (Peng et al 2012), spray-drying was proposed as a technically appropriate manufacturing process for drying nanocellulose suspensions.

Particle morphology and particle size distribution are two critical factors in determining properties of dried powders (wettability, stability, and cohesiveness or dispersability) and their applications in

\* Corresponding author

<sup>†</sup> SWST member

composites (Vehring 2007; Moczo and Pukanszky 2008). Different particle morphologies and sizes with desired physical properties can be generated by manipulating the spray-drying process parameters (Nandiyanto and Okuyama 2011). Generally, six unit operations are involved in a spray-drying process: 1) preconcentration of the liquid; 2) atomization; 3) dehydration in a stream of hot gas; 4) powder separation; 5) cooling; and 6) packaging. Among the six unit operations, four mainly determined the particle morphology: preconcentration of the liquid feed, atomization, hot air drying, and cyclone separation. Preconcentration of the feeding liquid to an appropriate viscosity is a required first step. Higher solids concentration of the suspension produces larger particle sizes. At the same time, the specific drying nature of a liquid, liquid viscosity, liquid density, and surface tension also influences the particle properties (Nukiyama and Tanasawa 1938; Kim and Marshall 1971; Kumar and Prasad 1971; Rizkalla and Lefebvre 1975; Lefebvre 1989; Walton and Mumford 1999; Schick 2006; Vehring 2007; Hede et al 2008). Phenomenological studies of spray-dried particles showed that morphologies were dependent on the type of materials: 1) spherical particles for most materials; 2) agglomerates for aluminum oxide; 3) hollow (skin-forming) particles for coffee; 4) mushroom cap-shaped particles for glycoprotein, etc. The mean droplet size increased with an increase in liquid viscosity and liquid surface tension and decreased as liquid density increased. Because the liquid suspension was pumped through the atomization system, design variables of the atomizer (liquid orifice diameter and nozzle angle) and the operating variables (liquid feed rate and gas flow rate) can be controlled to generate particles with different morphologies (Kim and Marshall 1971; Kumar and Prasad 1971; Hede et al 2008). The sprayed droplet size increased with increases in liquid feed rate and decreased as gas flow rate increased. However, all the studies were based on specific atomization systems. Different materials may perform differently with different atomizers. There is no agreement among researchers relating the variation of droplet size among process variables. Interactions among all the variables

make agreement impossible. As the atomized sprays flow along the drying chamber in contact with the hot gas, movement of moisture in the droplet may cause particles to inflate, distort, or shrink. Depending on the nature of the materials, the drying surface of the droplet may move faster or slower than the dissolved or suspended components. These behaviors contribute to the different mechanisms forming the dried particles (Vehring 2007). The last unit operation affecting droplet morphology is the cyclone separation. Very small particles can be aspirated to the exhaust or collected using an electrostatic precipitator.

Given a spray dryer with a pneumatic two-fluid atomization system, three operating variables mainly determine the dried particle morphology: 1) CNF suspension concentration; 2) liquid feed rate; and 3) gas flow rate. The overall goal of this study was to provide insight into the fundamentals of spray-drying nanocellulose suspensions. The objectives were 1) to produce the smallest particle size of CNF by manipulating the three process variables; and 2) to quantify the obtained particle morphology.

## EXPERIMENTAL

### Materials

Two CNF suspensions were studied: 1) a commercial product of nanofibrillated cellulose (NFC) suspension ARBOCEL MF40-10 at 10 wt % from J. Rettenmaier & Sohne GMBH+CO.KG (Rosenberg, Germany); and 2) a cellulose nanocrystal (CNC) suspension at 6.5 wt % from the USDA Forest Service, Forest Products Laboratory (Madison, WI). Spray-drying of CNF suspensions was conducted using a laboratory-scale dryer Mini Spray Dryer B-290 (Buchi, Switzerland). High-purity nitrogen gas was injected to form the suspension droplets.

### Experimental Design of Spray-Drying Cellulose Nanofibril Suspensions

Experiments were designed to evaluate effects of the three process parameters on particle morphology and particle size distribution: 1) gas

Table 1. Experimental design of spray-drying experiments and resulting outlet temperatures.

Experiment (sample name)	Spray-drying processing parameters			Outlet temperature (°C)	
	Gas flow rate (L/h)	Suspension feeding rate (mL/min)	Suspension concentration (wt %)	NFC	CNC
1	410	4.5	1	100	93
2	540	4.5	1	75	91
3	410	8.0	1	86	87
4	540	8.0	1	74	84
5	410	4.5	2	103	94
6	540	4.5	2	89	92
7	410	8.0	2	93	88
8	540	8.0	2	76	84

NFC, nanofibrillated cellulose; CNC, cellulose nanocrystals.

flow rate; 2) liquid feed rate; and 3) solid concentration of the liquid. A completely random design ( $2^3$  factorial arrangements of treatments) with eight experimental runs was carried out to evaluate the three process factors at two levels (Table 1). An identical inlet temperature of 175°C for the drying gas determined from an earlier study was used for all experiments. The disruption of liquid into small droplets by the injected gas (nitrogen) was dependent on the viscosity of the suspension. The nozzle may become clogged during spray-drying of an NFC suspension with solids concentration greater than 2 wt %. Therefore, solid concentrations of CNC used were 1 and 2 wt % in water. Temperatures of spray-dried particles exiting from the drying chamber (outlet temperature) for each drying experiment were recorded. Before drying, distilled water was added to the original two suspensions and mixed using a Speed Mixer (Flack Tek Inc., Landrum, SC) for 4 min at 2000 rpm to obtain final CNC and NFC suspension concentrations.

### Scanning Electron Microscopy

Scanning electron microscopy (SEM) studies on morphologies of dried samples were carried out using an AMR 1820 (AMRay Co., Bedford, MA) scanning electron microscope. All samples were sputter-coated with gold before microscopic observations were obtained. SEM images were taken at an accelerating voltage of 10 kV at various magnifications.

### Particle Morphology Analysis

Particle size distribution was characterized using a Morphologi G3S system (Malvern Instruments, Ltd., Malvern, Worcestershire, UK). Operation procedures were detailed in a previous study (Peng et al 2012). In this study, volumes of 3 and 5 mm<sup>3</sup> were used for CNC and NFC, respectively. A standard operating procedure was developed for all measurements. Five measurements were performed for each sample. Effects of the three process parameters on the mean circle equivalent (CE) diameter (Peng et al 2012) of the particles were evaluated through a one-way analysis of variance (ANOVA) with a 0.05 significance level. A statistical model was used to represent the mean value of the CE diameter of dried CNF particles.

$$Y_{ijkl} = \mu + \alpha_i + \beta_j + \gamma_k + (\alpha\beta)_{ij} + (\alpha\gamma)_{ik} + (\beta\gamma)_{jk} + (\alpha\beta\gamma)_{ijk} + e_{ijkl}$$

where  $i = 1, 2$ ;  $j = 1, 2$ ;  $k = 1, 2$ ; and  $l = 1, 2, 3, 4, 5$ .  $Y_{ijkl}$  is mean CE diameters of the particles measured.  $\mu$  is population mean CE diameter of the CNF particles. The effect of gas flow rate, liquid feeding rate, and solid concentrations on the population mean CE diameters of the particles are represented by  $\alpha_i$ ,  $\beta_j$ , and  $\gamma_k$ . Effects of the interactions between two of the three process parameters on the mean CE diameter are symbolized as  $(\alpha\beta)_{ij}$ ,  $(\alpha\gamma)_{ik}$ , and  $(\beta\gamma)_{jk}$ . The interaction effect among the three parameters on the CE diameter is represented by  $(\alpha\beta\gamma)_{ijk}$ . The errors in this model ( $e_{ijkl}$ ) were assumed to be independently, identically, and normally distributed. Additionally, high sensitivity (HS) circularity (the particle area divided by the perimeter square of the actual particle image) and aspect ratio (the ratio of the width to the length) of the particles are reported.

## RESULTS AND DISCUSSION

### Morphological Characterization of Dried Particles

Spray-drying of NFC suspensions formed fibrous and agglomerate particles (Fig 1). From previous

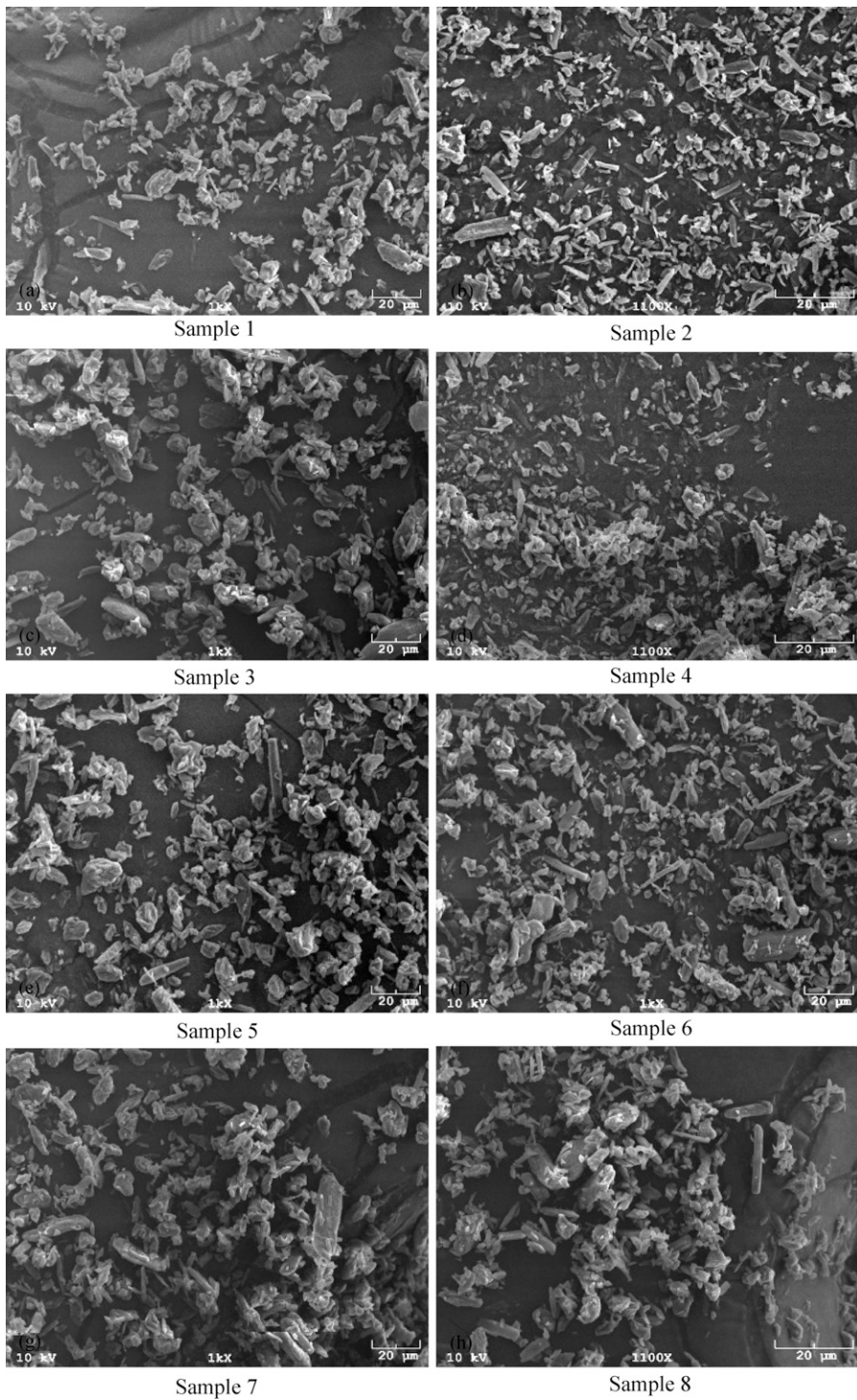


Figure 1. Scanning electron microscopy micrographs of spray-dried nanofibrillated cellulose as a function of different process parameters.

research (Peng et al 2012), NFC exhibiting both needle-like fibril shape and large cell wall sections (chunks) occurred in the original suspension. After spray-drying, single large cell wall sections were obtained separately (Fig 1b) in dry form particles with a width in the range of 2-4  $\mu\text{m}$  and length from 4-10  $\mu\text{m}$ . A few particles with lengths about 20  $\mu\text{m}$  were also observed (Fig 1). Morphology of the dried particles in this size range is mainly determined by the original particle size and morphology. Fibril particles with diameters about 300-400 nm were also observed in Fig 1. With different spray-drying parameters, different particle morphologies were obtained. For spray-drying conducted at the same liquid feed rate (4.5 mL/min) and solid concentration (1 wt %), most of the particles were separated fibrous materials under a higher gas flow rate 540 L/h (Sample 2 in Fig 1), whereas agglomerates and fibrous materials occurred for samples dried under a lower gas flow rate of 410 L/h (Sample 1 in Fig 1). Observations of Fig 1c-h indicated that different spray-drying parameters formed particles with various proportions of fibrous materials and agglomerates. More agglomerates appeared to be produced for suspensions dried at a higher liquid feed rate (8 mL/min) (Fig 1c, d, g, and h). More moisture needs to be evaporated per unit time at a higher liquid feed rate, causing the evaporation rate to decrease. Moisture content of the powders would increase, and more agglomerates would form. This hypothesis can be supported by examining outlet temperatures of the spray-dried particles. Under the same gas flow rate and solids concentration, the outlet temperature of the suspension dried with a higher liquid feed rate (8 mL/min) was lower than those dried at a lower liquid feed rate (4.5 mL/min) (Table 1). The outlet temperature is the maximum temperature the collected powders experienced during spray-drying. The lower the outlet temperature, the higher the residue moisture content of the dried particles.

SEM micrographs of the spray-dried CNC are shown in Fig 2. All the dried CNC particles exhibited similar morphology. Most particles were irregular with external voids. A small por-

tion of spherical particles is also discernible in each micrograph. In addition, the spherical particles were smaller than the irregular-shaped particles. The length of CNC particles is generally between several hundred nanometers to more than 10  $\mu\text{m}$ . Spherical particles were less than 1  $\mu\text{m}$  in size, whereas irregular-shaped particles ranged from 1 to more than 10  $\mu\text{m}$ . Some irregular particles had mushroom cap shapes (Fig 2e, g, and h), whereas some were doughnut-shaped with a bottom layer (Fig 2). Based on observations of the size and shape of the dried CNC, spherical particles were expected to be solid. The original CNC in aqueous suspension exhibited needle-like fibrils (Peng et al 2012). After spray-drying, the needle-like fibrils agglomerate to form spherical and irregular particles with minimum particle size equal to or greater than the length of original CNC fibrils. In some instances, small spherical particles were located inside the mushroom cap-shaped particles (Fig 2f-h). Consistent with drying NFC, the outlet temperature for drying CNC at the 8-mL/min feed rate was lower than those dried at a feed rate of 4.5 mL/min with the same gas flow rate and suspension solids concentration.

### Proposed Particle Formation Mechanisms

As the NFC suspension flowed through the atomization system, two different droplets were formed in the drying chamber (Fig 3). Because of the original size and morphology of the NFC fibrils in suspension, long and large cell wall sections coexisted with relatively short and skinny NFC fibrils (Peng et al 2012). For the first situation, the original length of NFC fibril was greater than the diameter of the formed droplet. At the same time, the NFC fibril was stiff enough to protrude outside the droplet (Fig 3). The other situation is that all the NFC fibrils were contained inside the droplet. In the second kind of droplets, a portion of the NFC fibrils may have been longer than the diameter of the droplet. However, these NFC fibrils were too soft to overcome the surface tension of water and they were folded within the droplet. While the NFC suspension droplets passed through the

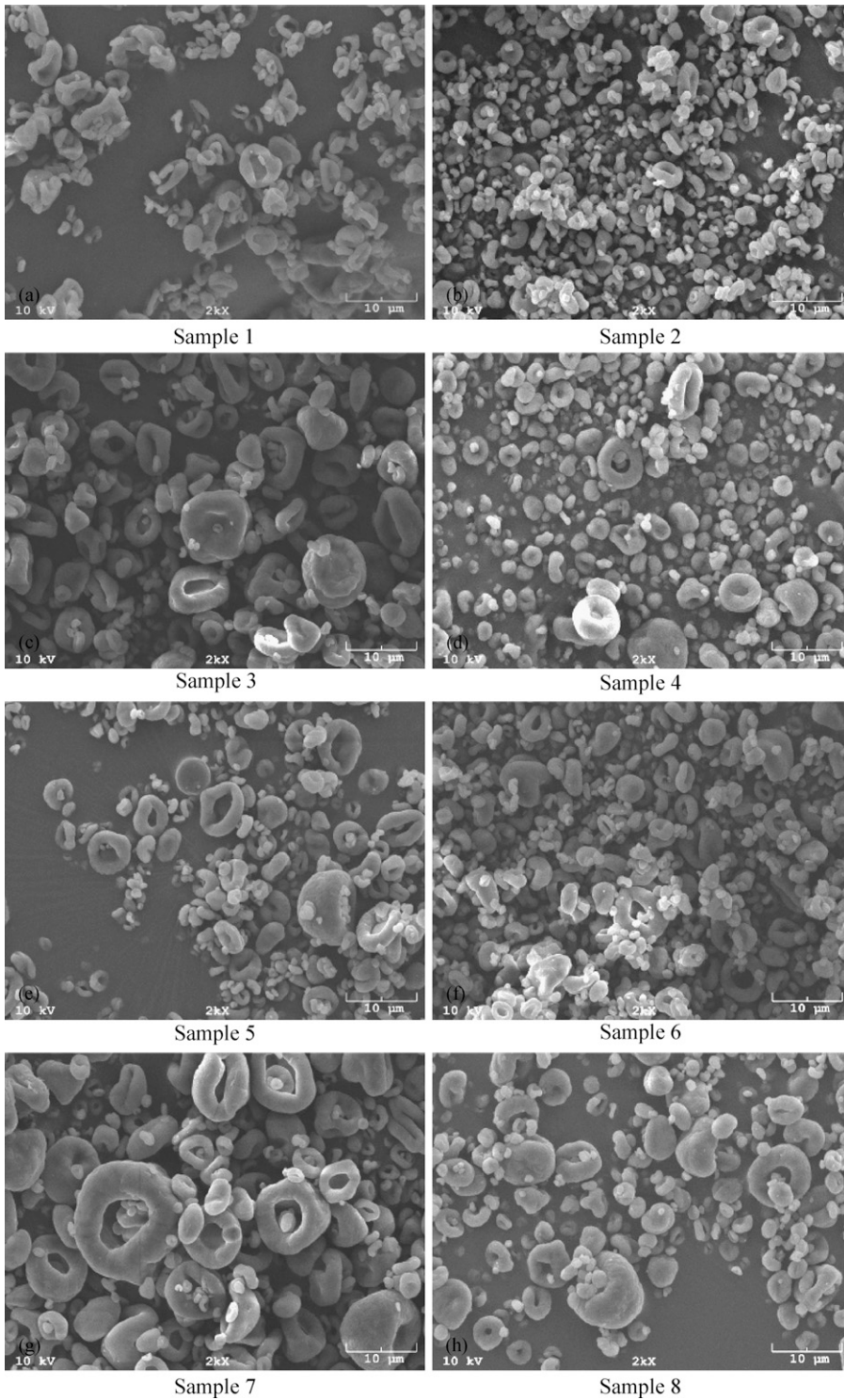


Figure 2. Scanning electron microscopy micrographs of spray-dried cellulose nanocrystals with different process parameters.

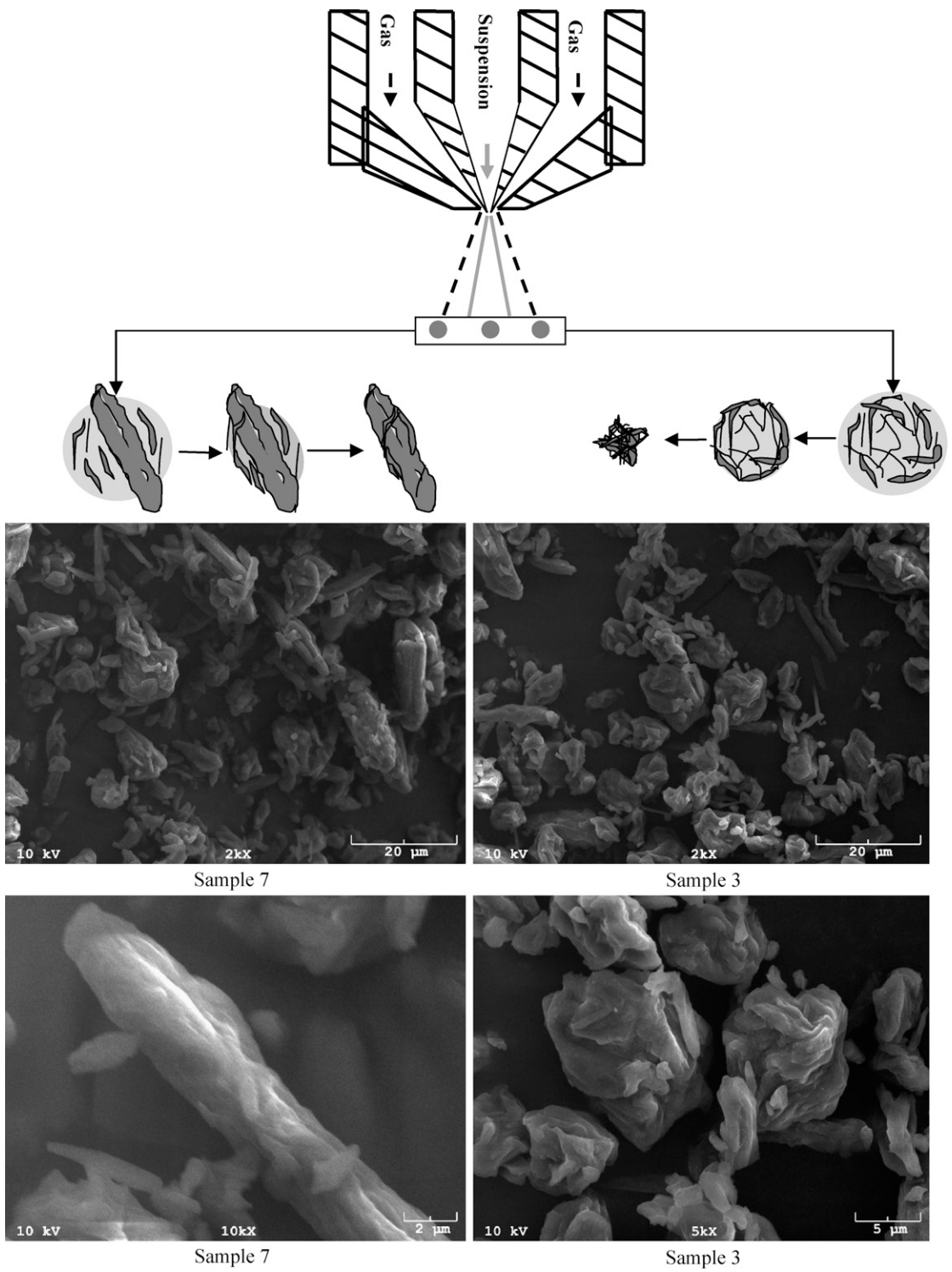


Figure 3. Nanofibrillated cellulose particle formation mechanism during spray-drying.

drying chamber in contact with hot gas, evaporation of water occurred. The evaporation process for a single suspension droplet was complex, involving several drying stages with different drying rates (Brinker and Scherer 1990; Scherer 1990; Mujumdar and Devahastin 2000). When NFC suspensions were dried at an inlet temperature of  $175^{\circ}\text{C}$ , the proposed droplet temperature history followed the gray line in Fig 4 based on the measured spray-drying outlet temperatures and related studies described in the literature (Farid 2003; Patel et al 2005; Handscomb et al 2009). At the same time, coupled with the increase in the temperature of NFC droplets, the gas temperature decreased from the inlet temperature ( $175^{\circ}\text{C}$ ) to the same temperature as the dried NFC droplet (black line in Fig 4). In the first stage (AB in Fig 4), the droplet containing NFC was heated rapidly to the wet bulb temperature. No evaporation occurred in this stage. Then the second stage of evaporation occurred at a constant rate (Phase BC in Fig 4). At this second stage (BC), the NFC droplet temperature was assumed to remain at the wet bulb temperature until the free water on the droplet surface was zero. Because of the free water evaporation, the droplet shrank and the size of the droplet decreased. With NFC fibrils contained inside, the surface of the spherical droplet became irregular because of the dissimilar shrinkage and dispersion of the NFC fibrils. As

evaporation proceeded, NFC concentration builds up on the surface, and they become closely packed or entangled. As a result, a crust (solid phase) was formed on the droplet surface and shrinkage of the droplet terminated (point C). The solid phase formed on point C also limited the water diffusion from inside the droplet to the surface, resulting in a decreased rate of drying. Spray-drying samples (2, 3, 4, 6, 7, and 8) were finalized during the third stage (CD) with the corresponding outlet temperatures  $75$ ,  $86$ ,  $74$ ,  $89$ ,  $93$ , and  $76^{\circ}\text{C}$ . When the droplet temperature continued to increase, the boiling temperature of water was approached and vaporization of water occurred inside the droplet. This was the situation for spray-drying of sample 1 with the outlet temperature of  $100^{\circ}\text{C}$ . The temperature profiles for this phase of NFC droplet and gas are shown as dotted lines in Fig 4. At this stage, the drying rate is controlled by the external heat transfer from gas to particle. In the last stage (EF in Fig 4), the particle temperature could further increase to the temperature of the surrounding gas (point F) if the gas temperature was higher than the boiling temperature. The existence of this fifth stage depended on the inlet temperature and process parameter settings of the spray-dryer. In this study, it is hypothesized that NFC sample 5 experienced the five drying stages with the outlet temperature of  $103^{\circ}\text{C}$  (dashed lines in Fig 4). With the different temperature histories, different morphologies of dried NFC particles occurred. Also, the solid particle size and the properties of the formed crust may have influenced the formed particle morphology (Walton and Mumford 1999; Vehring 2007; Handscomb et al 2009). When drying spherical NFC droplets, dimpled or wrinkled particles were formed (Figs 1 and 3). For droplets with long fibrils protruding, rod-like particles were formed with small fibrils adhering to the surface (Fig 3). With the same process parameters, spray-drying of the CNC suspensions formed particles with significantly different morphologies from those of NFC samples (Figs 1 and 2). This was partially caused by the different droplet temperature history between CNC and NFC droplets in the drying chamber. In spray-drying CNC

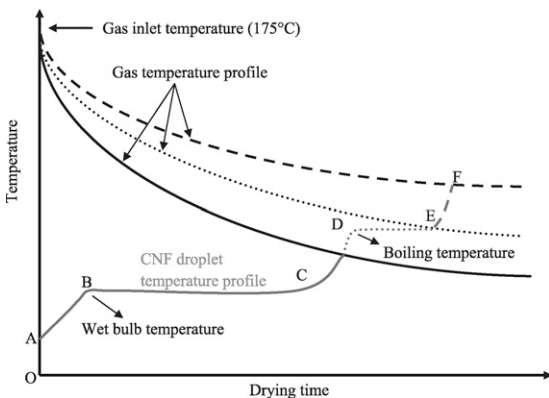


Figure 4. Temperature history for nanofibrillated cellulose and cellulose nanocrystal (CNC) droplets in the spray-drying chamber according to outlet temperatures.



suspensions, droplets may only experience the first three drying stages because the measured outlet temperatures for CNC samples were all below 100°C. The temperature profile with time for the CNC droplets is the gray solid line in Fig 4. Another main contribution to the different morphology between NFC and CNC was the much smaller size and narrower size distribution of CNC in the aqueous suspension compared with NFC. A single peak from 712-1484 nm was

observed for the NFC sample, whereas two peaks were obtained for the CNC sample: 1) from 24-44 nm; and 2) from 91-295 nm (Peng et al 2012). During droplet drying, only spherical droplets were formed after atomization of the CNC suspensions, and the smaller size of needle-shaped CNC fibrils could be easily rearranged inside the spherical droplet. This was not the case with the NFC droplets. NFC fibrils were easily entangled to resist the diffusion forces

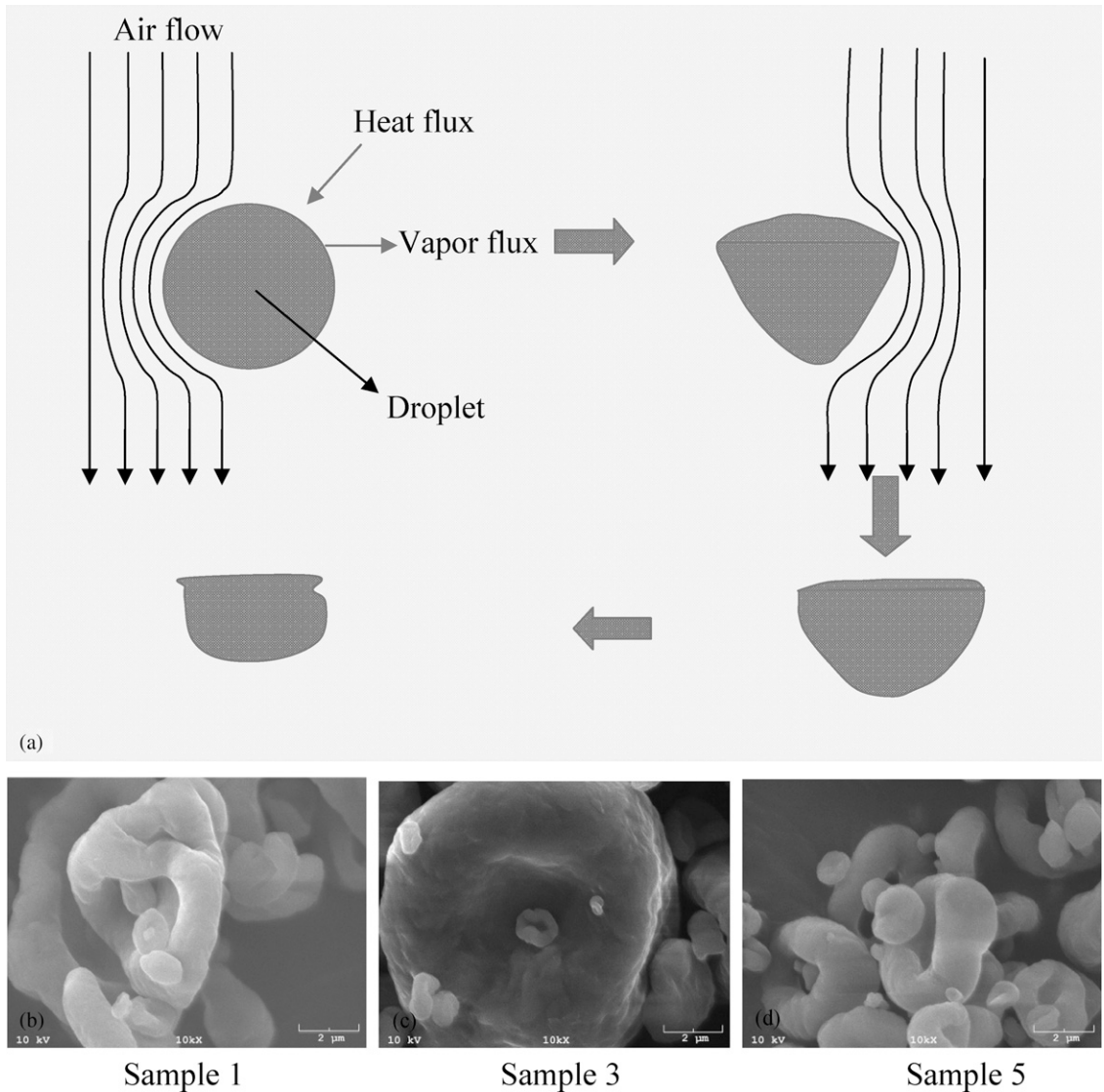


Figure 5. Demonstration of spray-drying of cellulose nanocrystal droplets.

Table 2. The CE diameter, HS circularity, and aspect ratio of spray-dried CNF.

Sample	CE diameter mean ( $\mu\text{m}$ )		HS circularity mean		Aspect ratio mean	
	NFC	CNC	NFC	NC	NFC	CNC
1	4.26 (0.24)	4.44 (0.22)	0.77 (0.03)	0.82 (0.01)	0.669 (0.011)	0.729 (0.006)
2	4.35 (0.47)	3.62 (0.09)	0.73 (0.03)	0.83 (0.01)	0.664 (0.007)	0.746 (0.003)
3	4.24 (0.09)	4.57 (0.21)	0.77 (0.02)	0.82 (0.02)	0.678 (0.007)	0.745 (0.007)
4	4.09 (0.22)	3.61 (0.15)	0.75 (0.02)	0.85 (0.01)	0.668 (0.011)	0.771 (0.008)
5	4.27 (0.14)	4.08 (0.20)	0.80 (0.01)	0.81 (0.06)	0.682 (0.005)	0.751 (0.008)
6	4.10 (0.33)	4.05 (0.10)	0.75 (0.01)	0.83 (0.01)	0.667 (0.009)	0.754 (0.003)
7	4.21 (0.10)	4.59 (0.24)	0.78 (0.01)	0.86 (0.01)	0.683 (0.004)	0.773 (0.004)
8	3.95 (0.28)	3.64 (0.05)	0.78 (0.02)	0.86 (0.01)	0.661 (0.007)	0.777 (0.005)

CE, circle equivalent; HS, high sensitivity; CNF, cellulose nanofibril; NFC, nanofibrillated cellulose; CNC, cellulose nanocrystals.

Table 3. One-way analysis of variance on mean circle equivalent (CE) diameter of nanofibrillated cellulose (NFC) and cellulose nanocrystals (CNC) samples.<sup>a</sup>

Source	Degree of freedom	Sum of squares		Mean square		F value		<i>p</i> value	
		NFC	CNC	NFC	CNC	NFC	CNC	NFC	CNC
Corrected total	39	2.7952	7.1960						
Model	7	0.5872	6.2525						
G	1	0.1525	4.7403	0.1525	4.7403	2.21	160.77	0.1469	<0.0001
F	1	0.1575	0.0276	0.1575	0.0276	2.28	0.93	0.1406	0.3409
C	1	0.1071	0.0081	0.1071	0.0081	1.55	0.28	0.2218	0.6033
G*F	1	0.0681	0.6996	0.0681	0.6996	0.99	23.73	0.3281	<0.0001
G*C	1	0.0856	0.3980	0.0856	0.3980	1.24	13.50	0.2738	0.0009
F*C	1	0.0031	0.0006	0.0031	0.0006	0.04	0.02	0.8345	0.8910
G*F*C#	1	0.0133	0.3783	0.0133	0.3783	0.19	12.83	0.6633	0.0011
Error	32	2.2080	0.9435	0.0690	0.0295				

<sup>a</sup> The three processing parameters are represented by G, gas flow rate, F, liquid feeding rate, and C, solids concentrations of cellulose nanofibril in suspensions.

associated with evaporation. By flowing along with the hot air in the drying chamber, an indentation on the top surface of the spherical CNC droplets was created by the dynamic air drag (Fig 5a) (Lane 1951) and mushroom cap-shaped and donut-shaped particles were obtained (Fig 2). At the same time, smaller particles were deposited into the larger particles via blowholes or craters, which were formed by the indentation on the top surface (Figs 2f-h and 5b-d). Although the spherical NFC droplets went through the same drying process, the entanglement of longer NFC fibrils in the droplet prevented the deformation caused by resistance to the airflow. No mushroom cap-shaped or donut-shaped particles occurred in the NFC samples.

### Particle Size Distribution

Statistical mean values of the CE diameter, HS circularity, and aspect ratio for the dried NFC

and CNC samples are shown in Table 2. The CE diameters of NFC and CNC were Gaussian distributed. HS circularity values indicate that the CNC particles more closely resembled a circle than those of NFC particles (A perfect circle has an HS circularity of 1, whereas an irregular object has an HS circularity value closer to 0). Also, aspect ratios of NFC samples were smaller than those of CNC samples. The one-way ANOVA calculations used to evaluate the effect of the three spray-drying process parameters on mean CE diameters of CNC and NFC samples are shown in Table 3. The results show that the three operating variables interacted to significantly affect the mean CE diameter of CNC samples ( $p = 0.0011$ ), whereas they did not interact to affect the mean CE diameter of NFC samples ( $p = 0.6633$ ). Mean CE diameters with different samples were compared for NFC and CNC, respectively (Fig 6). For NFC particles with the same gas flow rate of 540 L/h, spray-drying of a higher concentration

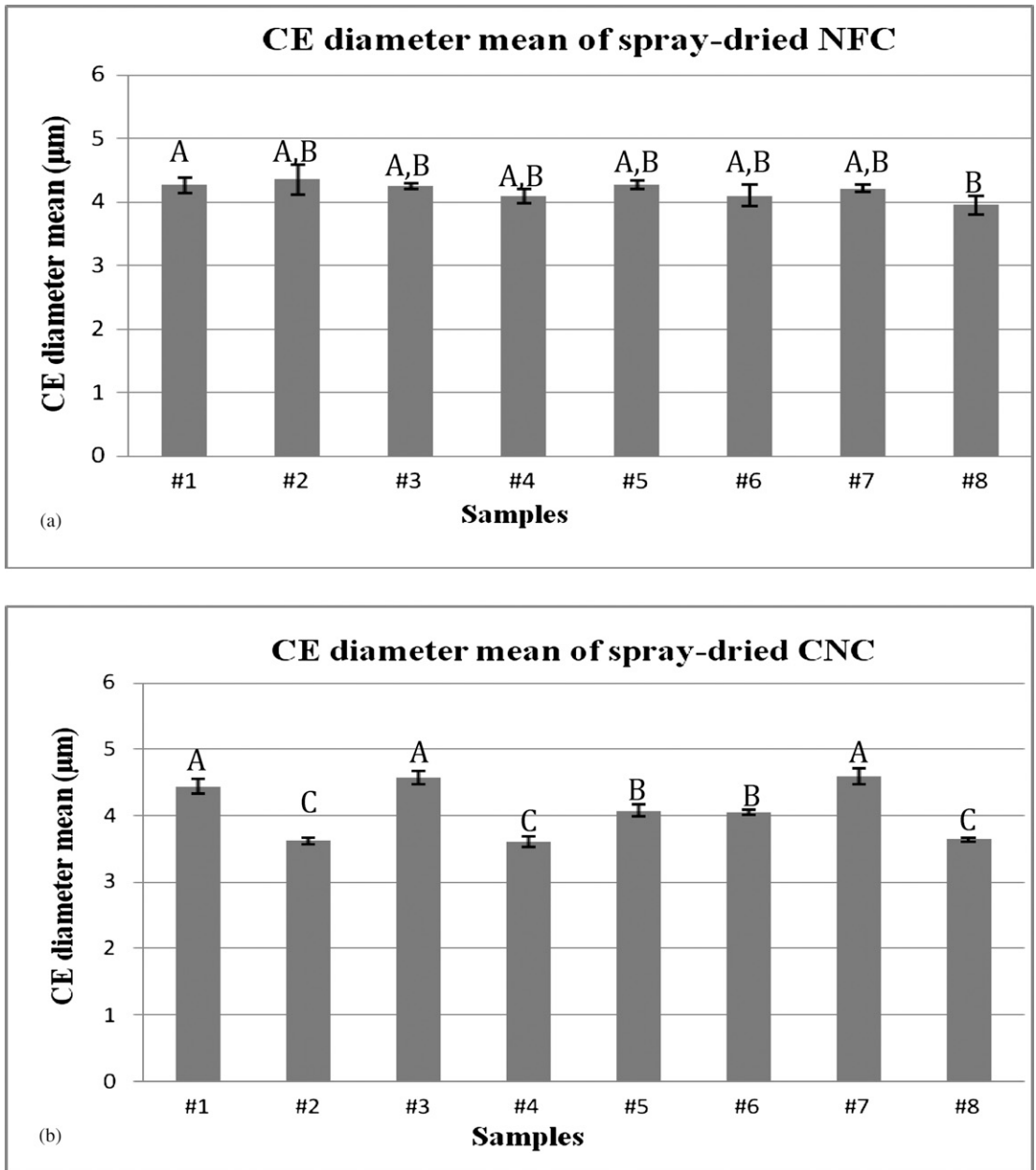


Figure 6. Comparison of mean circle equivalent (CE) diameters among (a) nanofibrillated cellulose (NFC) and (b) cellulose nanocrystal (CNC) samples with different process parameters. Capital letters A, B, and C in (a) and (b) represent significant differences among the CE diameters.

of NFC (2 wt %) suspension with higher liquid feeding rate (8 mL/min) produced particles (sample 8) with a significantly smaller mean CE diameter (3.95 μm) compared with drying

of lower (1 wt %) solids content of NFC suspensions at lower liquid feeding rate (4.5 mL/min) (4.35 μm for sample 2). According to spray-drying process literature (Rizkalla and Lefebvre

1975; Schick 2006; Hede et al 2008), an increase in liquid feeding rate and liquid viscosity (high solids concentration) should increase particle size. In this study, the opposite result was obtained. The interaction effect between liquid feeding rate and suspension concentration on particle size may contribute to this conflicting result. The conflicting result may also be mainly caused by the relatively large size of the original NFC fibrils in the suspension compared with the formed droplets through the spray dryer. This possibility can be demonstrated by the fact that no significant difference was observed for all the other samples produced with different spray-drying parameters. Another possible explanation is that the process parameters examined in this study were not varied enough to distinguish differences among the spray-dried NFC particles based on particle size characterization.

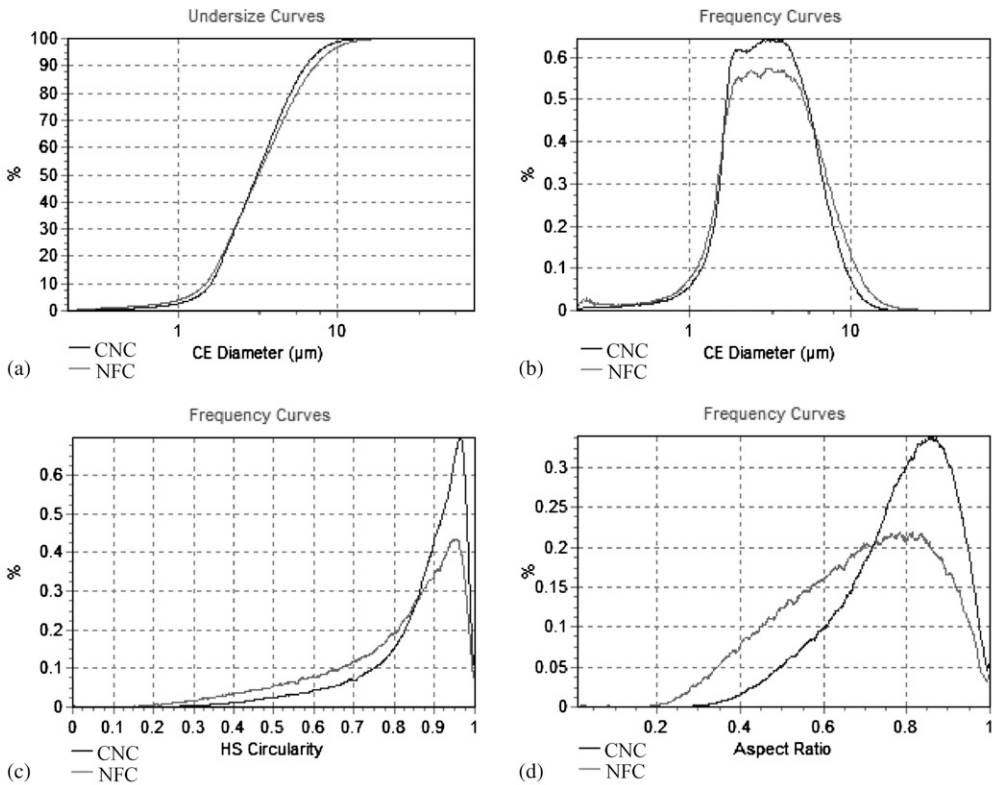
For the CNC samples, different spray-drying parameters resulted in different particle sizes. With the same suspension concentration and liquid feeding rate, the CE diameters of CNC particles produced at a gas flow rate of 540 L/h were significantly smaller than those dried at 410 L/h gas flow rate (Fig 6; Table 2). Higher gas flow rates should produce particles with smaller size (Lefebvre 1989; Hede et al 2008). The only exception was drying 2 wt % CNC suspensions at slower feeding rate (4.5 mL/min). No significant difference in the mean CE diameter was observed for drying such CNC suspensions at 410 and 540 L/h gas flow rate. The explanation for this exception is that the effect of suspension concentration and liquid feeding rate on the particle size may compensate for the effect of gas flow rate. No general trend was found for the effects of suspension solids content and feeding rate on the mean CE diameters of dried CNC particles. The interaction among the three operating variables made analysis of the spray-drying parameters complex. Each material required specific drying conditions to produce desired particle characteristics. Of all the factors influencing mean CE diameter of the dried CNF particles, gas flow rate appeared to be the most important. Following the analytical

results for the process parameters examined, the spray-drying parameter combination of 540 L/h gas flow rate, 8 mL/min liquid feeding rate, and 2 wt % solids concentration was proposed as the optimum processing condition for spray-drying of CNF suspensions. The smallest mean CE diameter can be obtained with these parameters in this study. Also, a higher solids concentration (2 wt %) and higher feeding rate (8 mL/min) could potentially increase the throughput of spray-drying CNF.

The statistical distribution curves for CE diameter, HS circularity, and aspect ratio from one measurement of CNC and NFC particles dried under the selected optimum process parameters are shown in Fig 7a-d. CE diameters of the NFC and CNC samples showed similar Gaussian distribution. The CNC particles exhibited a slightly narrower distribution for CE diameter than those of the NFC particles. The standard percentile readings  $D [n, 0.1]$ ,  $D [n, 0.5]$ , and  $D [n, 0.9]$  of the CE diameter derived from the statistical distribution were 1.60, 3.06, and 6.34  $\mu\text{m}$  for CNC, whereas the standard percentile readings for NFC samples were 1.52, 3.18, and 7.27  $\mu\text{m}$ . The surface- ( $D [3, 2]$ ) and volume-weighted ( $D [4, 3]$ ) means of the CE diameters of CNC and NFC are also documented in Fig 7e. Frequency curves of the HS circularity values, which were used to quantify how closely the particle shape resembles a circle, are indicated in Fig 7c. Number basis data of CNC and NFC showed a similar trend on HS circularity, whereas a larger volume of NFC was found to exhibit irregular shapes, matching the observations from the SEM micrographs. Aspect ratio distributions of the CNC and NFC samples are shown in Fig 7d. More particles of the NFC samples had a lower aspect ratio (irregularly fibrous shape) than those of the CNC samples.

## CONCLUSIONS

Effects of three spray-drying process parameters on morphology and particle size distribution of dried NFC and CNC were evaluated using SEM and a morphological analyzer. Spray-drying of



Sample	CE diameter (μm)					
	Mean	D [n, 0.1]	D [n, 0.5]	D [n, 0.9]	D [3,2]	D [4,3]
(e) NFC	3.95(0.28)	1.52(0.04)	3.18(0.22)	7.27(0.68)	8.63(0.70)	13.52(1.12)
CNC	3.64(0.05)	1.60(0.05)	3.06(0.12)	6.43(0.18)	6.29(0.32)	8.03(0.53)

Figure 7. Quantitative characterization of particle size of cellulose nanocrystal (CNC) and nanofibrillated cellulose (NFC) samples with proposed optimum spray-drying process parameters: number basis data of circle equivalent (CE) diameter (a, undersize curves and b, frequency curves), high sensitivity (HS) circularity (c, frequency curves), aspect ratio (d, frequency curves), and standard percentile readings of CE diameters based on number (e). Numbers in parentheses of (e) are standard deviation of five measurements.

NFC formed agglomerates and fibrous materials depending on the original fibril property in the formed droplets. Spray-dried CNC formed spherical and mushroom cap (or donut) -shaped particles because of the interaction between air-flow and droplets. The particle morphology and particle size depended on the drying nature of the materials. Statistical analysis showed that the three parameters interacted to significantly affect the particle size of CNC samples, whereas they did not interact to affect the particle size of NFC samples. Gas flow rate was the most

important impact factor influencing particle size. For CNC suspensions, a higher gas flow rate produced smaller particle sizes. This was not the case for the NFC suspensions. No obvious trend was obtained for the effect of liquid feeding rate and solids concentrations on CNF particle size. The particles with the smallest mean CE diameters produced in this study were 3.95 μm for NFC and 3.64 μm for CNC. The study of other methods to decrease the CNF particle size during the spray-drying process, such as using surfactants to decrease suspension liquid surface

tension and chemical modification to decrease CNF surface energy, is ongoing.

#### ACKNOWLEDGMENTS

We acknowledge the US Army Corps of Engineers, Engineering R&D Center, and the Maine Agricultural and Forestry Experiment Station McIntire-Stennis Project ME09615-06 for financial support. The content and information does not necessarily reflect the position of the funding agencies. Much appreciation goes to J. Rettenmaier & Söhne GMBH Company for donating the nanofibrillated cellulose and the USDA Forest Service Forest Products Laboratory for donating the cellulose nanocrystals. This is paper 3278 of the Maine Agricultural and Forest Experiment Station.

#### REFERENCES

- Beecher JF (2007) Organic materials: Wood, trees and nanotechnology. *Nat Nanotechnol* 2:466-467.
- Brinker CJ, Scherer GW (1990) Drying. Pages 453-513 in CJ Brinker and GW Scherer, eds. *Sol-gel science: The physics and chemistry of sol-gel processing*, 1st ed. Academic Press Limited, London, UK.
- Eichhorn SJ, Dufresne A, Aranguren M, Marcovich NE, Capadona JR, Rowan SJ, Weder C, Thielemans W, Roman M, Renneckar S, Gindl W, Veigel S, Keckes J, Yano H, Abe K, Nogi M, Nakagaito AN, Mangalam A, Simonsen J, Benight AS, Bismarck A, Berglund LA, Peijs T (2010) Review: Current international research into cellulose nanofibres and nanocomposites. *J Mater Sci* 45:1-33.
- Farid M (2003) A new approach to modeling of single droplet drying. *Chem Eng Sci* 58(13):2985-2993.
- Gardner DJ, Oporto GS, Mills R, Samir MASA (2008) Adhesion and surface issues in cellulose and nanocellulose. *J Adhes Sci Technol* 22:545-567.
- Habibi Y, Lucia LA, Rojas OJ (2010) Cellulose nanocrystals: Chemistry, self-assembly, and applications. *Chem Rev* 110:3479-3500.
- Handscorn CS, Kraft M, Bayly AE (2009) A new model for the drying of droplets containing suspended solids. *Chem Eng Sci* 64:628-637.
- Hede PD, Bach P, Jensen AD (2008) Two-fluid spray atomization and pneumatic nozzles for fluid bed coating/agglomeration purposes: A review. *Chem Eng Sci* 63:3821-3842.
- Hubbe MA, Rojas OJ, Lucia LA, Sain M (2008) Cellulosic nanocomposites: A review. *Bioresources* 3(3):929-980.
- Kim KY, Marshall WRJ (1971) Drop-size distributions from pneumatic atomizers. *AIChE J* 17(3):575-584.
- Klemm D, Kramer F, Moritz S, Lindstrom T, Ankerfors M, Gray D, Dorris A (2011) Nanocelluloses: A new family of nature-based materials. *Angew Chem Int Ed* 50:5438-5466.
- Kumar R, Prasad KSL (1971) Studies on pneumatic atomization. *Industrial and Engineering Chemistry Process Design and Development* 10(3):357-365.
- Lane WR (1951) Shatter of drops in streams of air. *Ind Eng Chem* 43:1312-1317.
- Lefebvre AH (1989) *Atomization and sprays*. Hemisphere Publishing Corporation, Washington, DC.
- Moczko J, Pukanszky B (2008) Polymer micro and nanocomposites: Structure, interactions, properties. *J Ind Eng Chem* 14:535-563.
- Moon RJ, Marini A, Nairn J, Simonsen J, Youngblood J (2011) Cellulose nanomaterials review: Structure, properties and nanocomposites. *Chem Soc Rev* 40:3941-3994.
- Mujumdar AS, Devahastin S (2000) Fundamental principles of drying. Pages 1-22 in S Devahastin, ed. *Mujumdar's practical guide to industrial drying*. Exergex Vorp., Montreal, Canada.
- Nandiyanto ABD, Okuyama K (2011) Progress in developing spray-drying methods for the production of controlled morphology particles: From the nanometer to submicrometer size ranges. *Advanced Powder Technology* 22:1-19.
- Nukiyama S, Tanasawa Y (1938) An experiment on the atomization of liquids by means of an air stream. *Trans Soc Mech Engrs (Japan)* 14(4):86-93.
- Patel KC, Chen XD, Kar S (2005) The temperature uniformity during air drying of a colloidal liquid droplet. *Drying Technol* 23:2337-2367.
- Peng Y, Gardner DJ, Han Y (2012) Drying cellulose nanofibrils: In search of a suitable method. *Cellulose* 19(1):91-102.
- Rizkalla AA, Lefebvre AH (1975) The influence of air and liquid properties on airblast atomization. *J Fluid Eng-T ASME* 97(3):316-320.
- Scherer GW (1990) Theory of drying. *J Am Ceram Soc* 73:3-14.
- Schick RJ (2006) *Spray technology reference guide: Understanding drop size*. Spray Analysis and Research Services, Spray Drying Systems Co. Wheaton, Illinois, USA. 35 pp.
- Siqueira G, Bras J, Dufresne A (2010) Cellulosic bionanocomposites: A review of preparation, properties and applications. *Polymers* 2:728-765.
- Siro I, Plackett D (2010) Microfibrillated cellulose and new nanocomposite materials: A review. *Cellulose* 17:459-494.
- Vehring R (2007) Pharmaceutical particle engineering via spray drying. *Pharm Res* 25(5):999-1022.
- Walton DE, Mumford CJ (1999) Spray dried products—Characterization of particle morphology. *Chem Eng Res Des* 77(1):21-38.